Materials Advances

ROYAL SOCIETY
OF **CHEMISTRY**

PAPER
G. J. Blanchard *et al*.
Layer-by-layer growth of graphene oxide multilayers using
robust interlayer linking chemistry. 1. Zr-bisphosphates

PAPER

Check for updates

Layer-by-layer growth of graphene oxide multilayers using robust interlayer linking chemistry. 1. Zr-bisphosphates

Neelanjana Mukherjee,[a] Nancy S. Muyanja[b] and G. J. Blanchard (ID) *[a]

Graphene oxide (GO) holds substantial interest because of its utility in applications ranging from chemical sensing to catalysis and energy storage. We report on the layer-by-layer formation of graphene oxide phosphate (P-GO) multilayers on silica and oxidized silicon supports, with the layers connected *via* Zr-bisphosphate (ZP) linking chemistry. Layers were grown either directly by ZP linkages between P-GO sheets, or with the use of 1,4-phenylene bisphosphate (BP1) or [1,1′-biphenyl]4,4′-diyl bisphosphate (BP2). The layers have been characterized using optical null ellipsometry, X-ray photoelectron spectroscopy (XPS), UV-visible absorption spectroscopy and scanning electron microscopy (SEM). There is a linear dependence of assembly thickness on the number of layers deposited and the integrated area of the optical absorbance bands also increases linearly with number of layers deposited. XPS data provides information on interlayer linking stoichiometry. SEM images provide insight into the morphology of the adlayers, suggesting the structure and length of the interlayer linking moieties used in the multilayer assembly play a significant role in the organization of the resulting system.

Introduction

The design and construction of layered interfaces has received significant attention for many years because of the potential value of such structures in applications, ranging from chemical sensing and separations to heterogeneous catalysis and molecular electronics.[1–6] While the application of micrometer-scale adlayers to surfaces has been established technology for more than a century, the formation of adlayers of molecular thickness, and the ability to deposit adlayers one layer at a time has been a very active area of research. The use of ultrathin layers for many applications holds great advantage for reasons of rapid diffusion, the ability to impart highly specific chemical functionality, and the separation of charge over nm or shorter distances. The design and fabrication of interfaces with molecular-layer control has been accomplished in a variety of ways, with the extent of molecular organization and the strength of adlayer bonding depending on the identity of the surface on which they are formed and the nature of the chemistry used to bond the adlayer to the interface.

The first practical method used to form monolayer structures was Langmuir–Blodgett deposition, where amphiphile monolayers were formed by lateral compression at the air–water interface and deposition onto support surfaces was accomplished by passing a support through the air–water interface at a controlled rate. The resulting adlayers were found to be ordered within the interface plane, but the strength of interaction within the layer and between the adlayer and the support surface was typically a few kcal mol^{-1} at best, insufficient to create a robust monolayer. Subsequent adlayer deposition techniques included siloxane adlayer growth, where the bonding of the adlayer to the interface was through covalent Si–O–Si bonds, but gaining control over adlayer thickness could be challenging.[7–10] Self-assembled monolayers of alkanethiols on coinage metal surfaces (mostly Au) allows for the formation of monolayers with the same level of order as that of the coinage metal surface,[11–21] and the strength of the adlayer bond to the metal surface was found to be on the order of $\sim$5 kcal mol^{-1}.[22] The reason for this modest binding energy was the enthalpically favored RS–Au bond formation was balanced against the entropic penalty associated with forming a 2-dimensional ordered array from a 3-dimensional solution.[23]

The Mallouk,[24–31] Thompson,[32] Page[33–35] and Katz[36–40] groups pioneered the growth of multilayer structures using metal bisphosphonate complexation chemistry to produce robust multilayered structures where the strength of the

[a] Department of Chemistry, Michigan State University, 578 S. Shaw Lane, East Lansing, MI 48824, USA. E-mail: blanchard@chemistry.msu.edu; Tel: +1 517 353 1105

[b] Michigan Center for Materials Characterization, College of Engineering, University of Michigan, Ann Arbor, MI 48109, USA

interlayer linkage could be on the order of 60 kcal mol^{-1} with Zr^{4+}.[41] Work by the Blanchard group utilized this interlayer linking chemistry to demonstrate layer-by-layer growth of maleimide-vinyl ether alternating copolymer systems, which exhibited chemical selectivity that depended on the identity of the polymer side groups and the order in which they were added in multilayer structures.[42–45] For these systems, the order within the adlayers was dominated by the morphology of the polymer, and to a lesser extent by the morphology of the support surface. The Blanchard group also demonstrated several covalent interlayer linking methods that produced robust multilayer structures with layer-by-layer control over the deposition process.[46–49]

Graphene oxide is a material that has found wide use because of its ability to function as a biocompatible material for bioelectrochemical applications,[50] as catalytic materials and for energy applications, such as supercapacitors and solar cells.[51] Graphene oxide materials display useful interfacial properties that allow efficient processing for nanocomposite manufacturing and enable stabilization and homogeneous distribution of metal nanoparticles along the carbon sheets, which is a necessity in heterogeneous catalysis and in energy-related applications. Key to the utility of graphene oxides in many applications is the ability to form interfacial assemblies where properties such as thickness can be controlled. In this paper, we report on the formation and characterization of graphene oxide (GO) multilayers *via* Zr-bisphosphate chemistry. The presence of several oxygen functionalities (alcohol, carboxylic acid, epoxide, carbonyl) on the surface of GO allows for the facile chemical modification of GO for its incorporation into comparatively well-controlled layered assemblies. The phosphorylation of GO reactive sites allows for the use of said materials in emerging nanoscale applications.[52]

Experimental section

Reagents and materials

Graphite, sodium nitrate (NaNO$_3$, $\geq$99.0%), sulfuric acid (H$_2$SO$_4$, 95.0–98.0%), potassium permanganate (KMnO$_4$, $\geq$99.0%), zirconyl chloride octahydrate (ZrOCl$_2$·8H$_2$O, 98%), anhydrous acetonitrile (CH$_3$CN anhydrous, 99.8%), phosphorous(v) oxychloride (POCl$_3$, 99%), 2,4,6-trimethylpyridine (collidine, 99.8%), hydroquinone ($\geq$99.5%), [1,1'-biphenyl]-4,4'-diol (97%) and ethanol ($>$99.5%) were purchased from Sigma-Aldrich. Hydrogen peroxide (H$_2$O$_2$, 30% in water) was purchased from Fisher Scientific. All reagents were used as received, without further purification. Silicon wafers were purchased from UniversityWafer Inc., South Boston, MA. Silica slides were purchased from UQG Ltd, Cambridge, UK. Ultrapure Milli-Q water (18 MΩ) was supplied by a Thermo Scientific Genpure system and used in all experiments. Glassware not used in anhydrous syntheses was rinsed with Milli-Q water before use.

GO synthesis and P-GO synthesis

GO was synthesized using a modified Hummers method.[53] Graphite (0.5 g) was mixed with 23 mL of sulfuric acid (conc.

reagent) in a beaker and stirred in an ice bath. NaNO$_3$ (0.5 g) was then added, followed by KMnO$_4$ (3 g). The mixture was brought to 35 °C and stirred for 2 h. The mixture was then cooled in an ice bath while 55 mL water was added slowly such that the temperature of the reaction mixture was maintained below 10 °C. Five mL of H$_2$O$_2$ (30% in water) was added slowly until gas evolution was no longer observed. Finally, the mixture was filtered under vacuum and the filter cake was redispersed in 25 mL of anhydrous CH$_3$CN. P-GO was synthesized from GO (in CH$_3$CN) by the addition of 234 μL of POCl$_3$ (0.2 M) and 325 μL (0.2 M) of collidine to the synthesized GO in a fume hood. The mixture was stirred for 10 minutes to ensure full mixing. The P-GO stock solution was covered with parafilm and was ready for use. The P-GO product was characterized by FTIR and the data matches that reported in the literature.[1] (Fig. S1 and S2)

Synthesis of BP1 and BP2 cross-linkers

1,4-Phenylene bisphosphate (BP1) was synthesized by the reaction of hydroquinone with POCl$_3$. The hydroquinone (0.2 mmol) was dissolved in anhydrous acetonitrile and was phosphated using 0.234 μL POCl$_3$ (0.2 mmol) and 0.325 μL collidine (0.2 mmol). [1,1'-biphenyl]-4,4'-diyl bis(dihydrogen phosphate) (BP2) was synthesized by the reaction of [1,1'-biphenyl]-4,4'-diol with POCl$_3$. The diol (0.2 mmol) was dissolved in anhydrous acetonitrile and was phosphated using 0.234 μL POCl$_3$ (0.2 mmol) and 0.325 μL collidine (0.2 mmol).

Surface preparation

Both silica and silicon substrates were cleaned in piranha solution (3 : 1 H$_2$SO$_4$: H$_2$O$_2$. Caution: strong oxidizer!) for 10 minutes, rinsed with Milli-Q water and dried under a stream of N$_2$ prior to layer deposition.

Layer deposition

The oxidized silicon and silica substrates were directly phosphated using POCl$_3$ and collidine in anhydrous acetonitrile in a fume hood. After 10 minutes, the substrates were rinsed with anhydrous acetonitrile and then immersed in Milli-Q water before use. The substrates were zirconated by immersion in a 5 mM solution of ZrOCl$_2$ in ethanol (aqueous, 60% v/v) for 1 minute (and 2 minutes). One minute immersion time proved to be as effective as longer immersion times and was used for subsequent layer growth. For P-GO layer formation, the zirconated substrates were immersed in the P-GO solution ($\sim$0.2 M) for 2 minutes (and 4 minutes). After immersion in P-GO solution, the resulting surfaces were washed with anhydrous acetonitrile, followed by water and dried with a stream of N$_2$ before characterization. The two different reaction times were studied to evaluate the role of immersion time on layer deposition. Multilayers that incorporated the interlayer spacers BP1 and BP2 were grown in a similar manner. Such layers were formed by dipping the phosphated substrates in ZrOCl$_2$ solution for one minute, then in 0.2 mM BP1 or BP2 in acetonitrile for one minute, then in ZrOCl$_2$ solution for one minute, then in P-GO solution for two (or four) minutes. Six layers were deposited for each type of multilayer assembly for
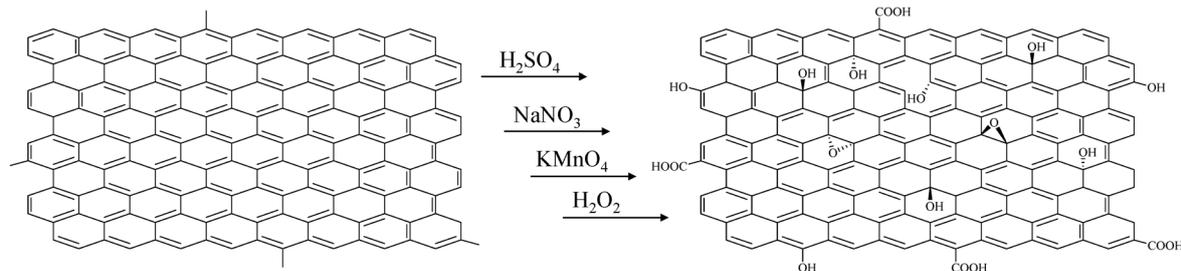
Fig. 1 Schematic of graphene oxide synthesis from graphene.

illustrative purposes. The formation of more than six layers would proceed in the same manner.

Optical null ellipsometry

Layer thicknesses were measured using an optical null ellipsometer (Woolam M-44, J. A. Woollam Co., Inc.). The instrument performs measurements at 44 discrete wavelengths in the range of 400 nm to 750 nm. The software used for data acquisition and reduction (WVASE32) was from the instrument manufacturer.

UV-visible spectroscopy

A Cary model 4000 UV-visible spectrometer was used to collect absorption spectra of the P-GO multilayer structures. Spectral resolution was 2 nm for all measurements.

X-Ray photoelectron spectroscopy

XPS data were acquired at the University of Michigan Center for Materials Characterization using a Kratos Axis Supra + system. The samples were probed with a monochromatic Al Kα X-ray beam at 1.486 keV with the anode tuned to 15 kV and 20 mA. Photoelectrons were collected from an area ∼700 μm × 300 μm at pass energies of 160 eV and 20 eV for survey and core scans respectively. The step size for spectral acquisition was set to 0.1 eV and 1 eV for core and survey scans respectively.

Scanning electron microscopy

A JEOL 7500F (field emission emitter) scanning electron microscope (JEOL Ltd, Tokyo, Japan) was used to collect SEM images at 5.0 kV accelerating voltage. SMILE VIEW Map software (developed by JEOL) was used for image processing and analysis. The samples were coated with osmium (∼10 nm thickness)

in a Tennant20 osmium chemical vapor deposition (CVD) coater (Meiwafosis Co., Ltd, Osaka, Japan), and were mounted on aluminum stubs using carbon suspension cement (SPI Supplies, West Chester, PA) and epoxy glue (System Three Quick Cure 5 from System Three Resins, Inc., Auburn, WA).

Results and discussion

We are interested in understanding the organization and structural properties of layered phosphated graphene oxide (P-GO) where the P-GO layers are bonded through zirconium-bisphosphate (ZP) coordination chemistry. There are several steps involved in the synthesis of such structures. The first step is the synthesis of GO from graphene, schematized in Fig. 1.

Following separation of the GO from the reaction vessel by filtration and washing with HCl(aq), the product is reacted with $POCl_3$ in acetonitrile, with collidine to replace the surface-bound -OH functionality with $-OPO_3^{-2}$. This reaction, schematized in Fig. 2, is required for multilayer growth.

With the P-GO synthesized, the silica or oxidized silica support surface is reacted to produce a phosphate-terminated surface. The reaction is between surface silanol functionalities and $POCl_3$ and it is shown in Fig. 3.

The phosphate-terminated surface is then reacted with Zr^{4+} to prime the support for reaction with P-GO, followed by exposure to P-GO. This sequence of reactions can be repeated to deposit multiple individual layers of P-GO (Fig. 4). The sequence of reactions shown in Fig. 4 form the basis for the layer-by-layer growth of P-GO. In addition to the formation of ZP linkages directly between P-GO "tiles", it is also a simple matter to control the interlayer spacing between P-GO tiles through the use of organobisphosphates, and we schematize
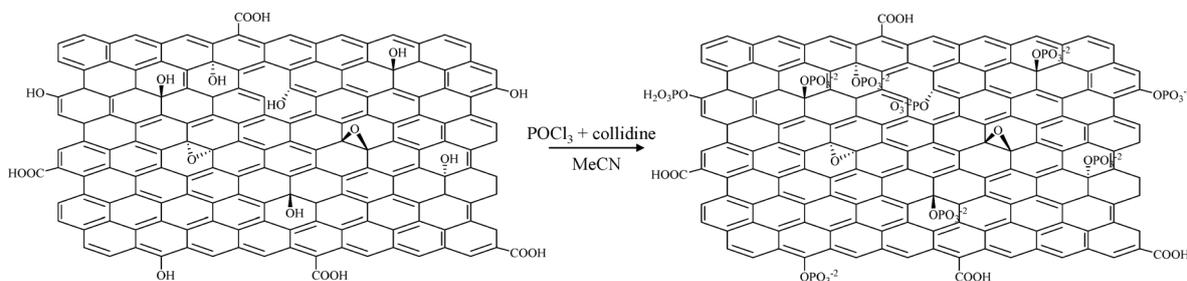

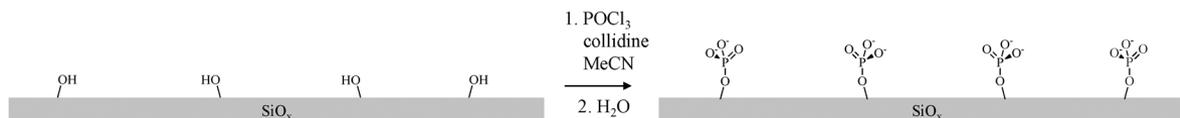**Fig. 2** Schematic of GO reaction with $POCl_3$ to form P-GO.

Fig. 3 Surface modification of silica or oxidized silicon surface with POCl$_3$ to produce a phosphate-terminated support surface.

this possibility in Fig. 5 for the spacer BP1. We also show in the inset to Fig. 5 the synthesis of spacers BP1 and BP2 from the diol precursors.

With the synthesis of the P-GO multilayers in hand, the next task is the characterization of the P-GO multilayers. The first order of business is to establish the formation of P-GO layers, and the ellipsometric thickness and optical absorption of the synthesized structures provide this information. The ellipsometric data (Fig. 6) provide information on the average layer thickness. P-GO multilayers exhibit a constant average layer thickness of 18.2 Å layer^{-1} for the Zr–P-GO system shown in Fig. 4, and 28.0 Å layer^{-1} for Zr–BP1–P-GO system and 33.7 Å layer^{-1} for Zr–BP2–P-GO system, shown in Fig. 5. In all cases, the thickness increases monotonically and linearly with increasing number of layers. These results are consistent with the structures of layer constituents and spacers; the length of the adlayer species is predicted by molecular mechanics to be 18 Å for Zr–P-GO layers, 28 Å for Zr–BP1–P-GO layers, and 34 Å for Zr–BP2–P-GO layers. While these data provide confidence in the regular growth of the adlayers, it is important to note that the ellipsometric data provide thickness results averaged over the spot size of the electric field used to perform the measurement (ca. 1 mm × 2 mm), and the correspondence between molecular mechanics expectations and the experimental data is consistent with the formation of uniform adlayers. Among the issues of concern is the speed of formation of the P-GO adlayers, and the data in Fig. 6a and b, for the growth of

P-GO adlayers with two minute and four minute reaction times exhibit the same slope. From these data we can conclude that the adlayer deposition kinetics are rapid for this system. This finding is fully consistent with earlier work on ZP multilayer growth using discrete molecules (e.g., BP1 or BP2) as layer constituents.

Measurement of the electronic spectra of the P-GO adlayers as a function of layer growth provide information complementary to ellipsometry data. The absorbance data and the integrated area under the absorbance bands from 183 nm to 450 nm for Zr–P-GO layers (2-minutes), from 183 nm to 800 nm for Zr–P-GO layers (4-minute exposure) and Zr–BP1–P-GO layers, and from 183 nm to 670 nm for the Zr–BP2–P-GO layers are shown in Fig. 7.

The integrated areas show a linear relationship between the integrated absorbance data and the number of layers deposited. This finding, along with the ellipsometric data, shows that there is full statistical monolayer coverage at each deposition on the substrates, consistent with the thickness expected for each layer based on molecular mechanics calculations. The band shape in the absorbance data for Zr–P-GO layers is different from that of the P-GO layers with the cross linkers. The difference in band shape for these two structural motifs suggests interlayer interactions between P-GO sheets when they are in sufficiently close proximity. The presence of the BP1 and BP2 cross-linkers appears to separate the P-GO layers sufficiently to render inter-layer interactions much less pronounced.
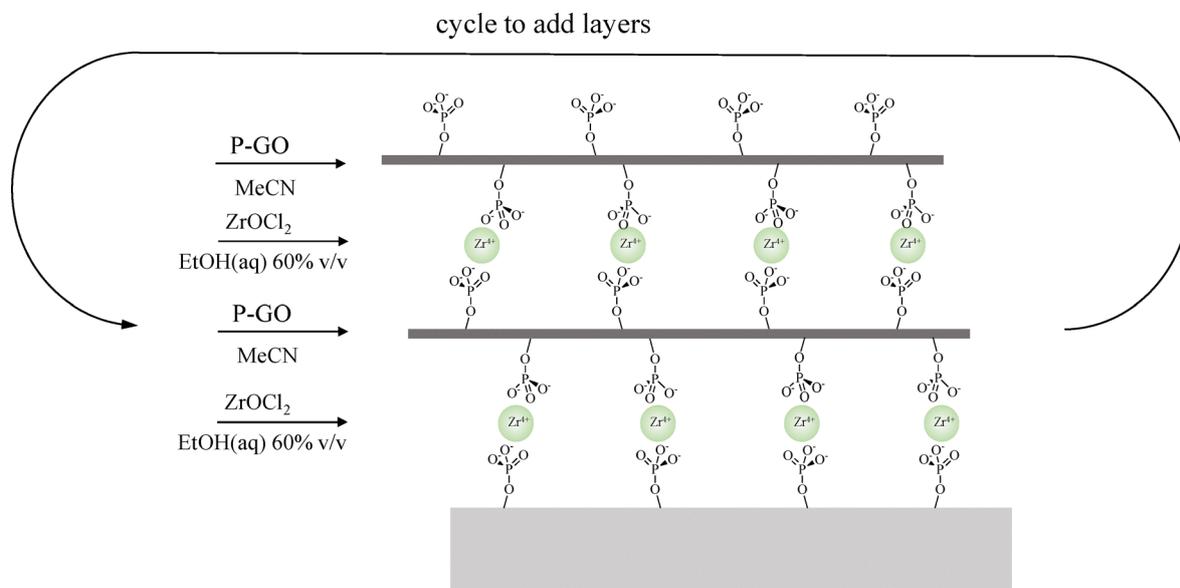

Fig. 4 Idealized reaction schematic of Phosphate-terminated silica surface with Zr^{4+} followed by exposure to P-GO. Two P-GO deposition cycles are shown.
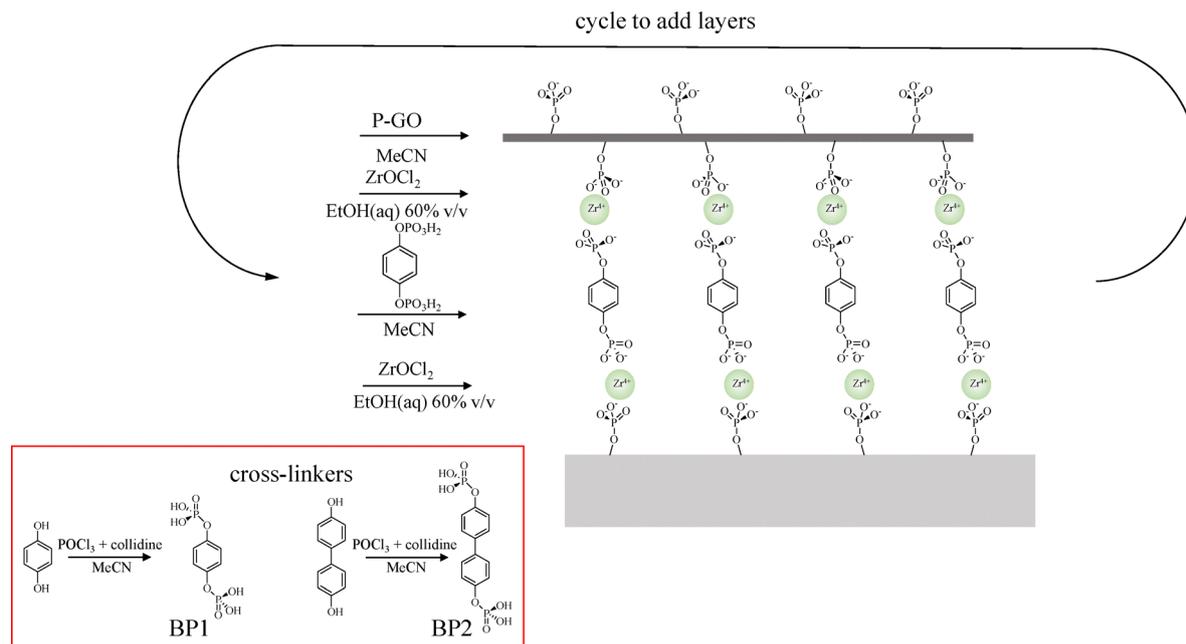
Fig. 5 Idealized reaction schematic to form P-GO layers, performed using interlayer spacers (BP1 shown). Inset: synthesis of spacers BP1 and BP2 from their diol precursors.
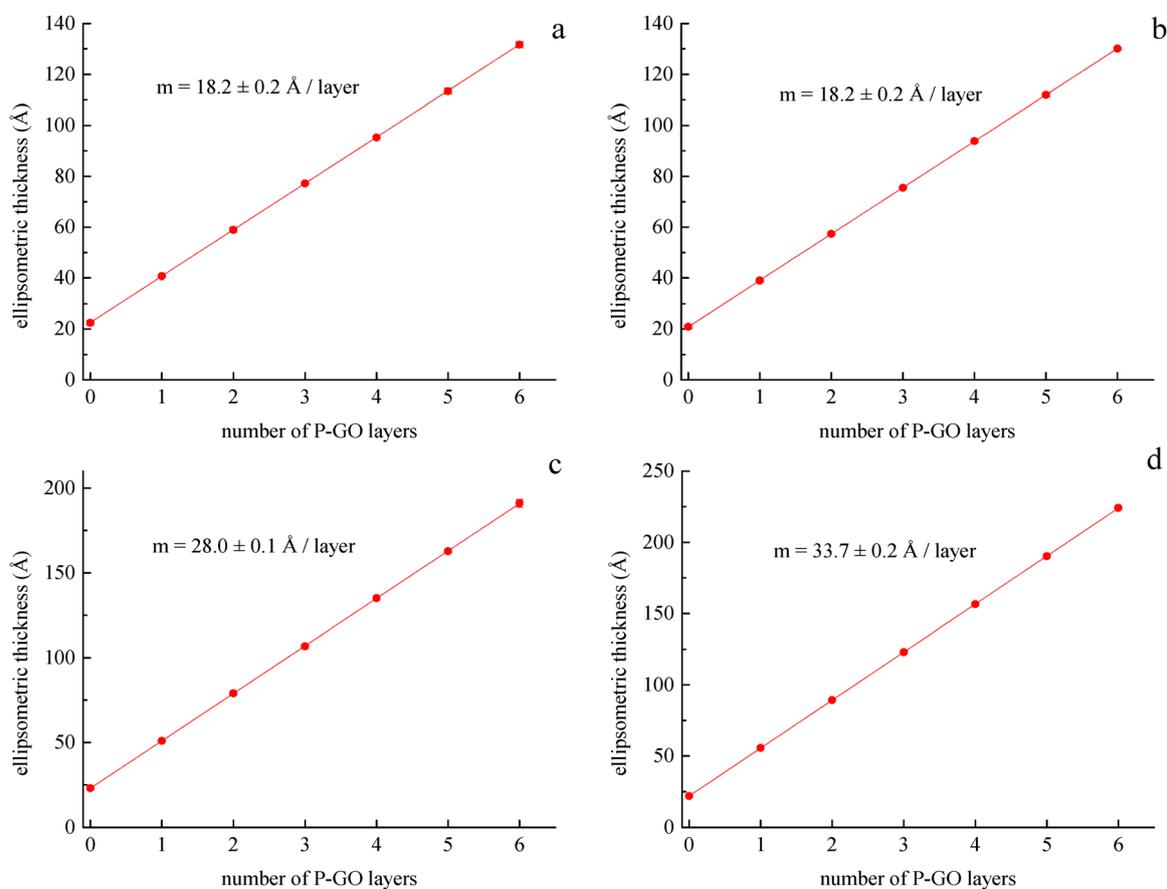

Fig. 6 Ellipsometric data for (a) P-GO layers bound through Zr^{4+} complexation (2 min reaction time), (b) P-GO layers bound through Zr^{4+} complexation (4 min reaction time), (c) P-GO layers with BP1 interlayer spacers, and (d) P-GO layers with BP2 interlayer spacers. The data reported are the average of 3 samples with typical uncertainties of 0.1–0.2 Å.
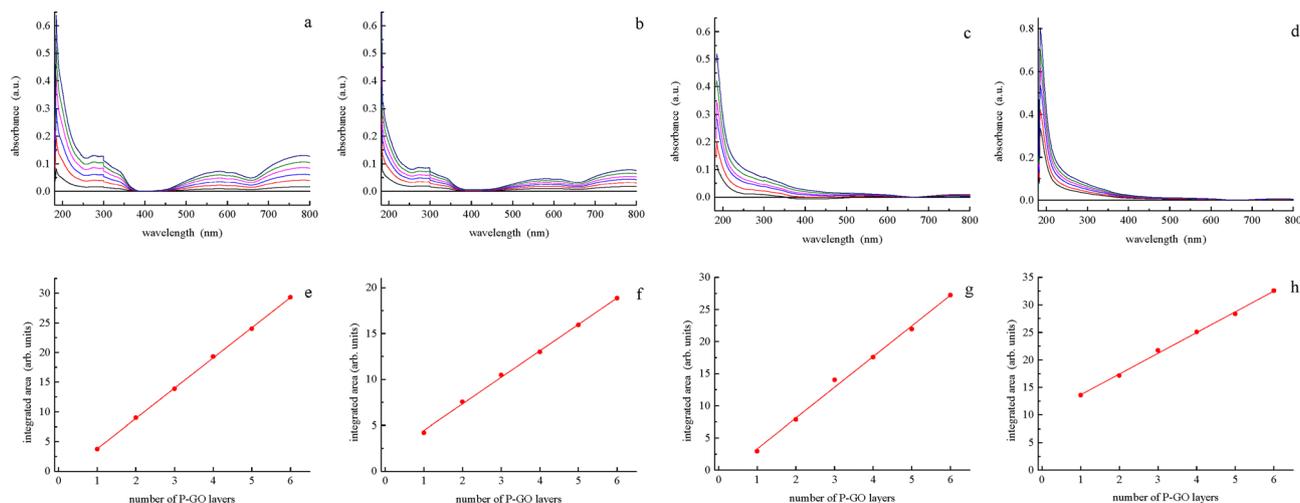
Fig. 7 Absorbance data and integrated areas P-GO layers bound through Zr^{4+} complexation (2 min reaction time, (a) and (e)); P-GO layers bound through Zr^{4+} complexation (4 min reaction time, (b) and (f)), P-GO layers with BP1 interlayer spacers (c) and (g), and P-GO layers with BP2 interlayer spacers (d) and (h).

Table 1 XPS atomic concentrations (%) for Zr, P, C and O. Uncertainties are $\pm 1\sigma$. XPS band assignments made using vendor software

Sample	Zr 3d	P 2p	C 1s	O 1s
1a	0.9 ± 0.1	2.6 ± 0.2	21.4 ± 0.3	29.0 ± 0.2
1b	1.3 ± 0.1	4.0 ± 0.2	12.2 ± 0.3	30.7 ± 0.2
2a	1.4 ± 0.1	4.4 ± 0.2	16.0 ± 0.3	30.0 ± 0.2
2b	1.1 ± 0.1	4.0 ± 0.2	22.8 ± 0.3	27.2 ± 0.2
Average	$1.1_8 \pm 0.2_0$	$3.7_5 \pm 0.4_0$	$18.1_0 \pm 0.6_0$	$29.2_3 \pm 0.4_0$

Further work and modeling is clearly indicated to understand from first principles the origin of these spectral features.

The ellipsometric and absorbance data both indicate the regular growth of P-GO adlayers with control over the interlayer spacing. The means of connection between the layers is Zr-bisphosphate linkages, and it is important to evaluate the stoichiometric relationship between Zr^{4+} and $-OPO_3^{2-}$. We have used XPS to make this comparison and present our results in Table 1. XPS spectra are shown in Fig. S3. From these data we find that the ratio of P : Zr is 3.2 ± 0.6, which is close to, but somewhat greater than one would expect based on the formal charges of Zr^{4+} and $-OPO_3^{-2}$. This finding is not surprising and is consistent with approximately half the Zr^{4+} being involved in the formation of a $Zr^{4+}(^-O_3PO-)_2$ interlayer linkages and half the Zr^{4+} being involved in complexation with only one phosphate functionality. This is not surprising because the location of the phosphate functionalities on the P-GO tiles is not likely to be regular, nor is the registration between layers. Thus, the observation that essentially half the Zr^{4+} in bisphosphate linkages is perhaps surprisingly high, and likely due to the strong driving force for the formation of the bisphosphate group. The Zr^{4+} that is associated with a single phosphate is likely to coordinate adventitious water efficiently, and that situation would give rise to a relatively high amount of oxygen in the XPS spectra.

With both the ellipsometric and optical absorbance data showing linear relationship with regular layer-by-layer growth, it is important to consider the morphology of these adlayers. Fig. 3 shows the SEM images of the adlayers. It is instructive to compare the images for the Zr–P-GO layers (Fig. 8a and b) for the two different reaction times. While the ellipsometric thickness and integrated absorbance data provide the same results in terms of layer thickness and growth, the morphology of the adlayers appears to be more uniform for the Zr–P-GO adlayers that were formed with a four minute reaction time, suggesting that the initial deposition process may be rapid but some time is required for structural annealing.

The images for the Zr–P-GO multilayers incorporating interlayer spacers BP1 and BP2 (Fig. 8c and d, respectively) reveal a more complex morphology. While further work is clearly required to elucidate the details of this morphology, it is possible that the presence of the interlayer spacers allows more conformational freedom in the interlayer linking process, and thus more apparent "relief" in the images.

Conclusions

We have designed and characterized 6 layers of phosphated graphene oxide using Zr-phosphonate chemistry. Optical ellipsometry and absorbance (the integrated areas under the peak) show step-by-step layer growth with layer thickness consistent with that expected from molecular mechanics calculations. The chemistry is spontaneous, as seen by the time scales used, and each layer can be formed by simple exposure to the P-GO solution for each layer. The SEM images show both the formation of tile-like layers, and homogenous layers. We anticipate that these multilayers will find utility in the design of chemically selective surfaces for various applications.
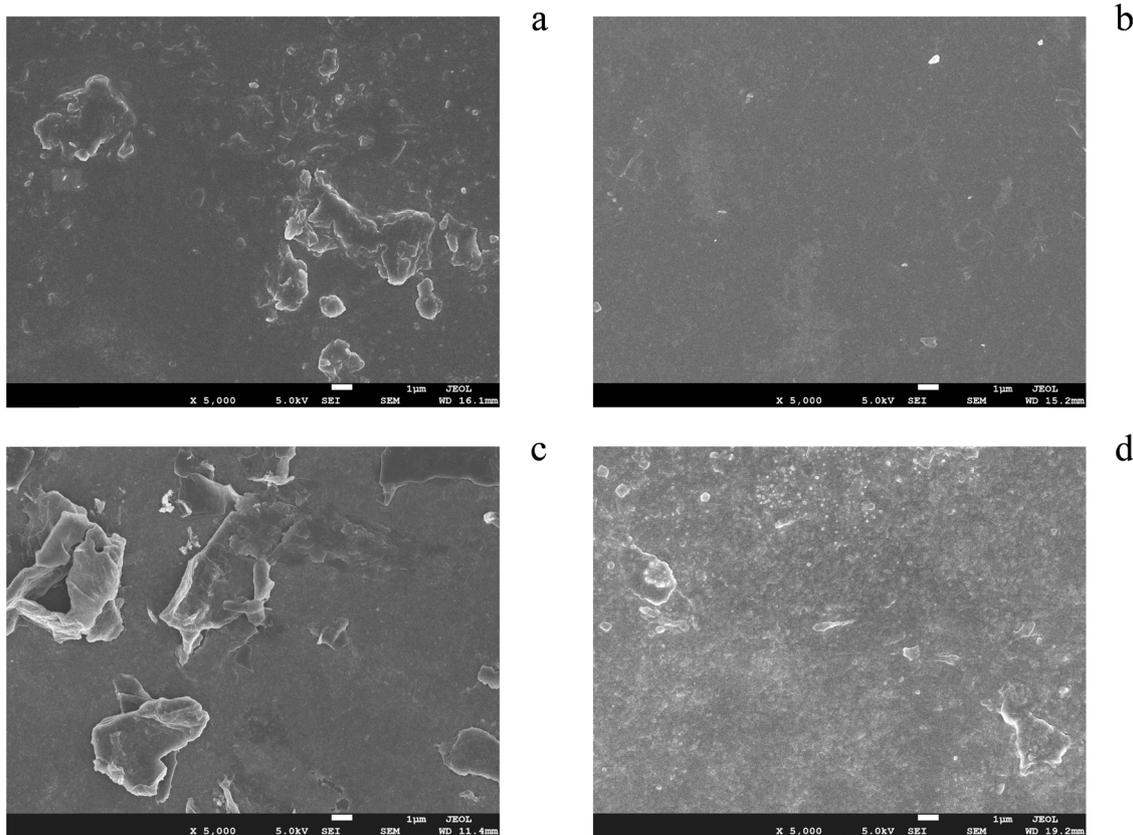
Fig. 8 SEM images (top view) of (a) Zr–PGO layers (2 min reaction time), (b) Zr–PGO layers (4 min reaction time), (c) PGO layers with BP1 interlayer spacers, and (d) PGO layers with BP2 interlayer spacers.

Conflicts of interest

There are no conflicts to declare.

Data availability

All data used in this work will be made available to any interested party. Please contact the corresponding author to obtain the data.

1. FTIR spectra of Graphene Oxide (GO) and Graphene Oxide Phosphate (P-GO). 2. Listing of relevant bands for P-GO in tabular format. 3. XPS survey scans of samples. See DOI: https://doi.org/10.1039/d5ma00600g.

Acknowledgements

References

1 W. Wang, X. Wang, Y. Pan, K. M. Liew, O. A. Mohamed, L. Song and Y. Hu, Synthesis of phosphorylated graphene oxide based multilayer coating: self-assembly method and application for improving the fire safety of cotton fabrics, *Ind. Eng. Chem. Res.*, 2017, **56**, 6664–6670.

2 Y. Cai, C. Wu, Z. Liu, L. Zhang, L. Chen, J. Wang, X. Wang, S. Yang and S. Wang, Fabrication of a phosphorylated graphene oxide–chitosan composite for highly effective and selective capture of U(vi), *Environ. Sci.: Nano*, 2017, **4**, 1876–1886.

3 H. Chen, Y. Wang, W. Zhao, G. Xiong, X. Cao, Y. Dai, Z. Le, Z. Zhang and Y. Liu, Phosphorylation of graphehe oxide to improve adsorption of U(vi) from aquaeous solutions, *J. Radioanal. Nucl. Chem.*, 2017, **313**, 175–189.

4 L. Sun, L. J. Kepley and R. M. Crooks, Molecular interactions between organized, surface-confined monolayers and vapor-phase probe molecules: hydrogen-bonding interactions, *Langmuir*, 1992, **8**, 2101–2103.

5 H. C. Yang, D. L. Dermody, C. Xu, A. J. Ricco and R. M. Crooks, Molecular Interactions between organized, surface-confined monolayers and vapor-phase probe molecules. 8. reactions between acid-terminated self-assembled monolayers and vapor-phase bases, *Langmuir*, 1996, **12**, 726–735.

6 M. Wells, D. L. Dermody, H. C. Yang, T. Kim, R. M. Crooks and A. J. Ricco, Interactions between organized, surface-confined monolayers and vapor-phase probe molecules. 9. structure/reactivity relationship between three surface-confined isomers of mercaptobenzoic acid and vapor-phase decylamine, *Langmuir*, 1996, **12**, 1989–1996.

7 L. Netzer and J. Sagiv, A new approach to construction of artificial monolayer assemblies, *J. Am. Chem. Soc.*, 1983, **105**, 674–676.

8 N. Tillman, A. Ulman and T. L. Penner, Formation of multilayers by self-assembly, *Langmuir*, 1989, **5**, 101–111.

9 Y. Liu, M. L. Bruening, D. E. Bergbreiter and R. M. Crooks, Multilayer Dendrimer–Polyanhydride Composite Films on Glass, Silicon, and Gold Wafers, *Angew. Chem., Int. Ed. Engl.*, 1997, **36**, 2114–2116.

10 P. Kohli, K. K. Taylor, J. J. Harris and G. J. Blanchard, Assembly of covalently-coupled disulfide multilayers on gold, *J. Am. Chem. Soc.*, 1998, **120**, 11962–11968.

11 C. D. Bain, E. B. Troughton, Y. T. Tao, J. Evall, G. M. Whitesides and R. G. Nuzzo, Formation of monolayer films by the spontaneous assembly of organic thiols from solution onto gold, *J. Am. Chem. Soc.*, 1989, **111**, 321–335.

12 C. D. Bain and G. M. Whitesides, Molecular-level control over surface order in self-assembled monolayer films of thiols on gold, *Science*, 1988, **240**, 62–63.

13 C. E. D. Chidsey, M. D. Porter and D. L. Allara, Electrochemical Characterization of *N*-alkyl thiol, sulfide, and disulfide monolayers on gold, *J. Electrochem. Soc.*, 1986, **133**, C130.

14 L. H. Dubois, B. R. Zegarski and R. G. Nuzzo, The chemisorption of organosulfur compounds on gold surfaces - construction of well-defined organic-solids, *J. Vac. Sci. Technol., A*, 1987, **5**, 634–635.

15 S. D. Evans and A. Ulman, Surface-potential studies of alkyl-thiol monolayers adsorbed on gold, *Chem. Phys. Lett.*, 1990, **170**, 462–466.

16 R. G. Nuzzo, F. A. Fusco and D. L. Allara, Spontaneously organized molecular assemblies. 3. preparation and properties of solution adsorbed monolayers of organic disulfides on gold Surfaces, *J. Am. Chem. Soc.*, 1987, **109**, 2358–2368.

17 M. D. Porter, T. B. Bright, D. L. Allara and C. E. D. Chidsey, Spontaneously organized molecular assemblies. 4. structural characterization of normal-alkyl thiol monolayers on gold by optical ellipsometry, infrared-spectroscopy, and electrochemistry, *J. Am. Chem. Soc.*, 1987, **109**, 3559–3568.

18 L. Strong and G. M. Whitesides, Structures of self-assembled monolayer films of organosulfur compounds adsorbed on gold single-crystals - electron- diffraction studies, *Langmuir*, 1988, **4**, 546–558.

19 J. D. Swalen, D. L. Allara, J. D. Andrade, E. A. Chandross, S. Garoff, J. Israelachvili, T. J. McCarthy, R. Murray, R. F. Pease, J. F. Rabolt, K. J. Wynne and H. Yu, Molecular monolayers and films, *Langmuir*, 1987, **3**, 932–950.

20 E. B. Troughton, C. D. Bain, G. M. Whitesides, R. G. Nuzzo, D. L. Allara and M. D. Porter, Monolayer films prepared by the spontaneous self-assembly of symmetrical and unsymmetrical dialkyl sulfides from solution onto gold substrates – structure, properties, and reactivity of constituent functional-groups, *Langmuir*, 1988, **4**, 365–385.

21 G. M. Whitesides, E. B. Troughton, C. Bain, S. R. Holmesfarley, S. R. Wasserman and L. H. Strong, Self-assembled organic monolayer films - organic sulfur- compounds on gold and related systems, *J. Electrochem. Soc.*, 1987, **134**, C110.

22 D. S. Karpovich and G. J. Blanchard, Direct measurement of the adsorption-kinetics of alkanethiolate self-assembled monolayers on a microcrystalline gold surface, *Langmuir*, 1994, **10**, 3315–3322.

23 H. M. Schessler, D. S. Karpovich and G. J. Blanchard, Quantitating the balance between enthalpic and entropic forces in alkanethiol/gold monolayer self assembly, *J. Am. Chem. Soc.*, 1996, **118**, 9645–9651.

24 C. M. Bell, S. W. Keller, V. M. Lynch and T. E. Mallouk, New solids and surfaces, via coordination chemistry, *Mater. Chem. Phys.*, 1993, **35**, 225–232.

25 G. Cao, H. G. Hong and T. E. Mallouk, Layered metal phosphates and phosphonates: from crystals to monolayers, *Acc. Chem. Res.*, 1992, **25**, 420–427.

26 G. Cao, L. K. Rabenberg, C. M. Nunn and T. E. Mallouk, Formation of quantum-size semiconductor particles in a layered metal phosphonate host lattice, *Chem. Mater.*, 1991, **3**, 149–156.

27 H. G. Hong, D. D. Sackett and T. E. Mallouk, Adsorption of well-ordered zirconium phosphonate multilayer films on high surface area silica, *Chem. Mater.*, 1991, **3**, 521–527.

28 H. Lee, L. J. Kepley, H. G. Hong, S. Akhter and T. E. Mallouk, Adsorption of ordered zirconium phosphonate multilayer films on silicon and gold surfaces, *J. Phys. Chem.*, 1988, **92**, 2597–2601.

29 H. Lee, L. J. Kepley, H. G. Hong, S. Akhter and T. E. Mallouk, Adsorption of ordered zirconium phosphonate multilayer films on silicon and gold surfaces, *J. Phys. Chem.*, 1988, **92**, 2597–2601.

30 H. Lee, L. J. Kepley, H. G. Hong and T. E. Mallouk, Inorganic analogs of Langmuir-Blodgett films: adsorption of ordered zirconium 1,10-decanebisphosphonate multilayers on silicon surfaces, *J. Am. Chem. Soc.*, 1988, **110**, 618–620.

31 H. C. Yang, K. Aoki, H. G. Hong, D. D. Sackett, M. F. Arendt, S. L. Yau, C. M. Bell and T. E. Mallouk, Growth and characterization of metal(II) alkanebisphosphonate multilayer thin films on gold surfaces, *J. Am. Chem. Soc.*, 1993, **115**, 11855–11862.

32 M. E. Thompson, Use of layered metal phosphonates for the design and construction of molecular materials, *Chem. Mater.*, 1994, **6**, 1168–1175.

33 M. A. Ansell, E. B. Cogan, G. A. Neff, R. von Roeschlaub and C. J. Page, Self-assembly of thin film superstructures based on alternating metal-bisphosphonate and cobalt diisocyanide layers, *Supramol. Sci.*, 1997, **4**, 21–26.

34 J. T. Obrien, A. C. Zeppenfeld, G. L. Richmond and C. J. Page, Fourier-transform infrared-spectroscopy studies of hafnium alkylbis(phosphonate) multilayers on gold -

effects of alkylbis(phosphonate) chain-length, substrate roughness, and surface functionalization on film structure and order, *Langmuir*, 1994, **10**, 4657–4663.

35 A. C. Zeppenfeld, S. L. Fiddler, W. K. Ham, B. J. Klopfenstein and C. J. Page, Variation of layer spacing in self-assembled hafnium-1,10- decanediylbis(phosphonate) multilayers as determined by ellipsometry and grazing angle x-ray-diffraction, *J. Am. Chem. Soc.*, 1994, **116**, 9158–9165.

36 H. E. Katz, Multilayer deposition of novel organophosphonates with zirconium(IV), *Chem. Mater.*, 1994, **6**, 2227–2232.

37 H. E. Katz, S. F. Bent, W. L. Wilson, M. L. Schilling and S. B. Ungashe Synthesis, Layer assembly, and fluorescence dynamics of poly(phenylenevinylene) oligomer phosphonates, *J. Am. Chem. Soc.*, 1994, **116**, 6631–6635.

38 H. E. Katz, G. Scheller, T. M. Putvinski, M. L. Schilling, W. L. Wilson and C. E. D. Chidsey, Polar orientation of dyes in robust multilayers by zirconium phosphate-phosphonate interlayers, *Science*, 1991, **254**, 1485–1487.

39 H. E. Katz, M. L. Schilling, C. E. D. Chidsey, T. M. Putvinski and R. S. Hutton, Quaterthiophenediphosphonic acid (QDP): a rigid, electron-rich building block for zirconium-based multilayers, *Chem. Mater.*, 1991, **3**, 699–703.

40 H. E. Katz, W. L. Wilson and G. Scheller, Chromophore structure, second harmonic generation, and orientational order in zirconium phosphonate/phosphate self-assembled multilayers, *J. Am. Chem. Soc.*, 1994, **116**, 6636–6640.

41 P. Kohli, M. C. Rini, J. S. Major and G. J. Blanchard, Elucidating the balance between metal ion complexation and polymer conformation in maleimide vinyl ether polymer multilayer structures, *J. Mater. Chem.*, 2001, **11**, 2996–3001.

42 P. Kohli and G. J. Blanchard, Design and growth of robust layered polymer assemblies with molecular thickness control, *Langmuir*, 1999, **15**, 1418–1422.

43 P. Kohli and G. J. Blanchard, Design and demonstration of hybrid multilayer structures: Layer-by-layer mixed covalent and ionic interlayer linking chemistry, *Langmuir*, 2000, **16**, 8518–8524.

44 P. Kohli and G. J. Blanchard, Applying polymer chemistry to interfaces: layer-by-layer and spontaneous growth of covalently bound multilayers, *Langmuir*, 2000, **16**, 4655–4661.

45 P. Kohli and G. J. Blanchard, Probing interfaces and surface reactions of zirconium phosphate/phosphonate multilayers using P-31 NMR spectrometry, *Langmuir*, 2000, **16**, 695–701.

46 J. S. Major and G. J. Blanchard, Covalently bound polymer multilayers for efficient metal ion sorption, *Langmuir*, 2001, **17**, 1163–1168.

47 J. S. Major and G. J. Blanchard, Acid-enhanced interfacial polymer layer growth, *Chem. Mater.*, 2002, **14**, 4320–4327.

48 J. S. Major and G. J. Blanchard, Strategies for covalent multilayer growth. 1. Polymer design and characterization, *Chem. Mater.*, 2002, **14**, 2567–2573.

49 J. S. Major and G. J. Blanchard, Achieving thermodynamic control of adsorption and desorption at layered polymer interfaces, *Langmuir*, 2003, **19**, 2267–2274.

50 O. Schlesinger and L. Alfonta, in *Methods in Enzymology*, ed. C. V. Kumar, Academic Press, 2018, vol. 609, pp. 197–219.

51 S. Yadav, A. P. Singh Raman, H. Meena, A. G. Goswami Bhawna, V. Kumar, P. Jain, G. Kumar, M. Sagar, D. K. Rana, I. Bahadur and P. Singh, An update on graphene oxide: applications and toxicity, *ACS Omega*, 2022, **7**, 35387–35445.

52 A. Anouar, N. Katir, A.-S. Mamede, A. Aboulaich, K. Draoui, S. Royer and A. El Kadib, Synthesis and multifaceted use of phosphorylated graphene oxide: growth of titanium dioxide clusters, interplay with gold nanoparticles and exfoliated sheets in bioplastics, *Mater. Chem. Front.*, 2019, **3**, 242–250.

53 W. S. HummersJr and R. E. Offeman, Preparation of Graphitic Oxide, *J. Am. Chem. Soc.*, 1958, **80**, 1339.